THE JOURNAL OF PHYSICAL CHEMISTRY Letters

Letter

pubs.acs.org/JPCL

Charge Redistribution at GaAs/P3HT Heterointerfaces with Different Surface Polarity

Jun Yin,[†] Dmitri B. Migas,[‡] Majid Panahandeh-Fard,[†] Shi Chen,[†] Zilong Wang,[†] Paola Lova,[†] and Cesare Soci*[,†,§]

[†]Division of Physics and Applied Physics, School of Physical and Mathematical Sciences and [§]Centre for Disruptive Photonic Technologies, Nanyang Technological University, 21 Nanyang Link, Singapore 637371

[‡]Belarusian State University of Informatics and Radioelectronics, 6 P. Browka Str., Minsk 220013, Belarus

Supporting Information

ABSTRACT: The nature of charged photoexcitations at the interface of highly delocalized inorganic crystals and more localized conjugated polymer systems is of great fundamental interest for a number of hybrid photovoltaic applications. Here we study the interaction between mainstream compound semiconductor GaAs and conjugated polymer P3HT by means of density functional theory simulations. When considering both nonpolar GaAs(110) and polar GaAs(111)B surfaces, we find that polarity of the GaAs surface strongly affects the electronic orbitals and charge redistribution: electrons are efficiently transferred to GaAs substrates, implying the formation of hybrid delocalized states at the interface. Furthermore, P3HT can act as an "acceptor" for GaAs(111)B via hole transfer from GaAs valence band states. Overall the intrinsic surface dipole moment of GaAs surfaces is enhanced by the charge displacement induced by adsorbed P3HT. These theoretical predictions correlate well with energy alignments derived by ultraviolet photoelectron spectroscopy and provide a robust methodology for the design of polymer/III−V heterointerfaces that optimize photovoltaic performance.

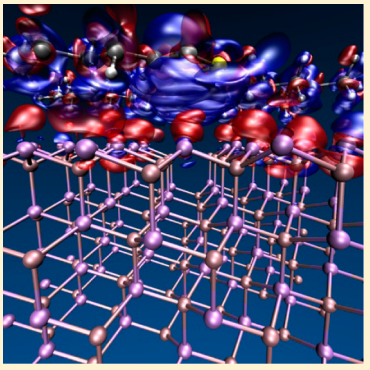

SECTION: Physical Processes in Nanomaterials and Nanostructures

Organic−inorganic hybrid photovoltaic (PV) systems, for instance, conjugated polymers blended with functionalized inorganic nanoparticles or nanorods,[1,2] offer great flexibility for the design of solar cells with large power conversion efficiency (PCE).[3−5] The overall photocurrent of hybrid PVs is primarily affected by the competition between interfacial charge separation and charge recombination.[6] Typically, the energy alignment between the conjugated polymer and the inorganic semiconductor is chosen so that the inorganic semiconductor acts as electron acceptor, facilitating dissociation of the photogenerated excitons and preventing charge recombination.[7] These processes depend strongly on the atomic configurations and electronic structures at the interface as well as on the electronic coupling between the polymer and the semiconductor substrate.[8] The nature of charged photoexcitations at the interface of highly delocalized inorganic crystals and more localized, disordered conjugated systems is indeed of great fundamental interest but not yet completely understood.[9−13]

GaAs, a mainstream III−V compound semiconductor with high carrier mobility and direct bandgap absorption well-overlapped with the solar irradiance, is rapidly emerging as exceptional PV material for thin film technologies,[14] including dye or polymer sensitized hybrid solar cells.[15−18] Early demonstration of a hybrid PV cell based on a quaterthiophene/GaAs bilayer yielded 1.7% PCE;[15] more recently, use of GaAs nanowires blended either in P3HT bulk heterojunctions[16] or in a bilayer thin-film configuration[17,19] allowed achieving PCEs of >2.3 and 9.2%, respectively.

Despite very promising device performances, current understanding of the electronic properties leading to charge transfer at organic−inorganic interfaces like GaAs/P3HT is relatively limited.[20] For instance, the effects of surface polarity on charge redistribution and the nature of hybrid excitations formed upon charge transfer between highly delocalized electronic states of the crystal, and less extended states of the polymer are unknown. In this work, we investigate the structural and electronic properties of thin P3HT films deposited on polar GaAs(111)B and nonpolar GaAs(110) substrates. First-principle, total-energy calculations are used to study the orientation and position of P3HT molecules at the different interfaces and to determine stable atomic configurations. Density of states and charge density rearrangement due to the formation of the interface suggests the formation of hybrid states upon photoexcitation. Calculated electronic energy structure at the GaAs/P3HT interfaces and electronic coupling between GaAs surfaces and the P3HT molecules display a good agreement with X-ray photoelectron spectroscopy (XPS) and ultraviolet photoelectron spectroscopy (UPS) experimental

Received: July 15, 2013
Accepted: September 17, 2013
Published: September 17, 2013

   dx.doi.org/10.1021/jz401485t | J. Phys. Chem. Lett. 2013, 4, 3303−3309

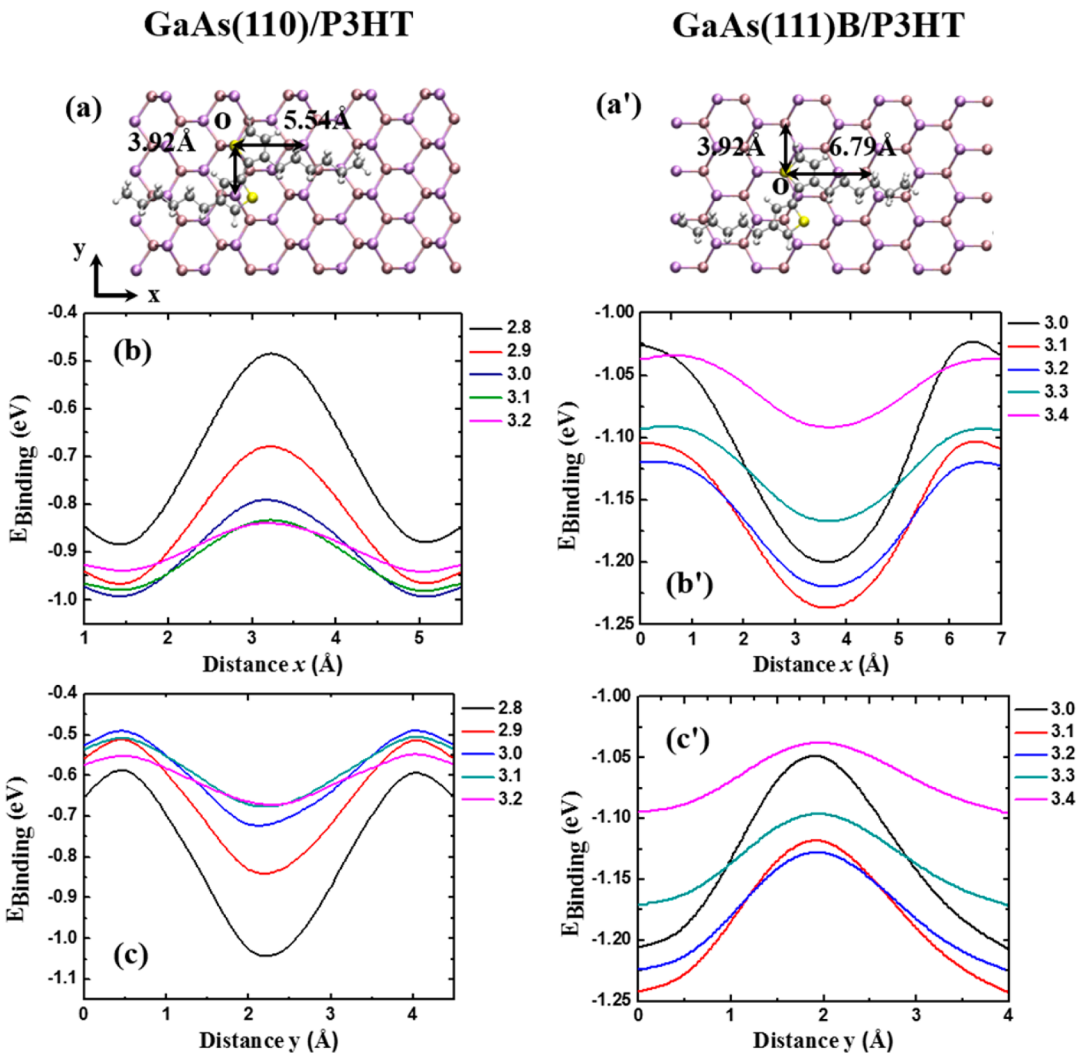

Figure 1. Geometrical optimization of P3HT adsorbed on GaAs surfaces: top views of the optimized geometry of P3HT on GaAs(110) (a) and on GaAs(111)B (a′); binding energy of a P3HT molecule on GaAs(110) (b,c) and on GaAs(111)B (b′,c′) surfaces as a function of its relative position along the x and y axes.

results. Finally, contributions of ground-state charge-transfer processes for different surface polarities are identified, indicating that electron and hole accumulation layers may be engineered, controlling the GaAs crystal orientation to optimize PV performance.

DFT simulations proceeded through the optimization of the structural conformations of P3HT crystal in contact with GaAs surfaces, followed by full atomistic relaxation to determine electronic couplings and finally the charge density redistribution after electron and hole transfer. After structural optimization, the polar GaAs(111)B surface shows stable alignment of the outmost layer, while the nonpolar GaAs(110) surface experiences a strong reorganization of the outmost layer, where As and Ga atoms display outward and inward relaxation, respectively. This is in good agreement with previous calculations.[21,22] Surface relaxation causes the enlargement of Ga−As bonds in the GaAs(111)B surface bilayer (from 2.400 to 2.417 Å) and the reduction of Ga−As bonds in the GaAs(110) surface bilayer (from 2.400 to 2.375 Å). Similar to the known case of ZnO/P3HT interface, we assume that van der Waals interactions of thiophene π band and side-chain force physisorbed P3HT molecules to lay flat on the GaAs surface. Dag et al.[23] have shown that the LDA method accurately describes ZnO and P3HT interactions, although it somehow fails accounting for long-range van der Waals attractive components. Here we also adopt the LDA method to model the interactions between the GaAs surface and P3HT, but instead of calculating a large and thick GaAs supercell with P3HT polymer interfacial system, we use the outmost bilayer of the GaAs surface to represent the original GaAs surface and two repeated P3HT molecules to represent the polymer, a common approach to study the bonding energy of organic/inorganic interfaces.[23,24] The most stable adsorption sites of the P3HT molecule on GaAs(110) and GaAs(111)B bilayer surfaces are shown in Figure 1a,a′. Structural optimization was carried out through various energy minimization steps: at first, the stable interfacial distances between the P3HT molecular plane and the GaAs(110) and GaAs(111)B bilayer surface were determined to be ∼3.10 and 2.95 Å, respectively. (These distances correspond to the minima of the binding energy curves provided as Supporting Information, Figure S1.) Then, the most stable configurations along the x and y axes were found to be at x = 1.5 Å and y = 2 Å for GaAs(110) (Figures 1b,c) and x = 3.5 Å and y = 0 Å for GaAs(111B) (Figures 1b′,c′) while the optimal rotational angle in the x−y plane was 0° (Figure S2 in the Supporting Information). Therefore, for

dx.doi.org/10.1021/jz401485t | J. Phys. Chem. Lett. 2013, 4, 3303−3309

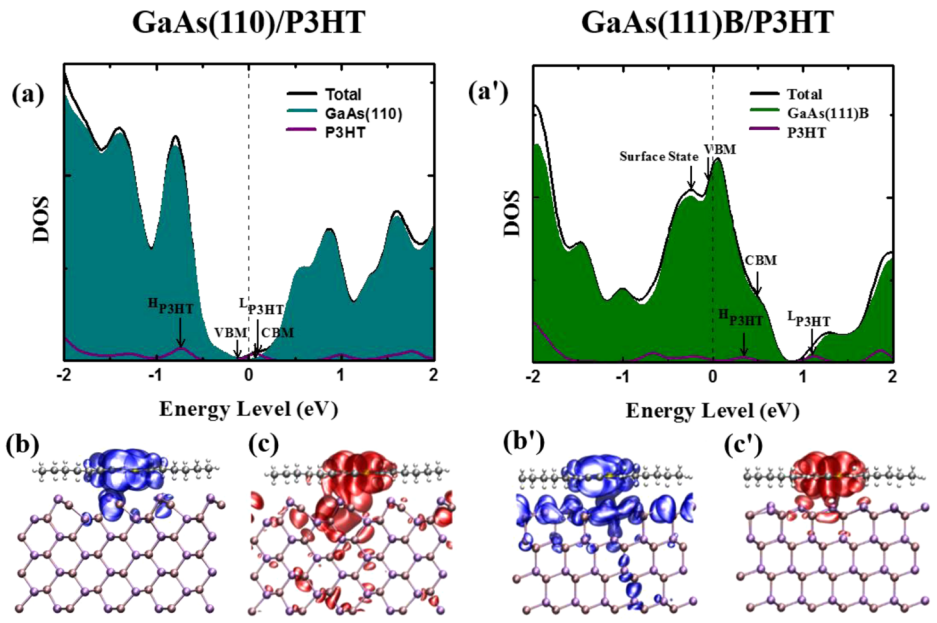

Figure 2. Density of states and electronic orbital distribution in GaAs(110)/P3HT (left) and GaAs(111)B/P3HT (right) hybrid systems: (a,a′) density of states (the dashed line indicates the position of the Fermi energy); charge distribution of the electron (b,b′); and hole (c,c′) orbitals.

both GaAs surfaces the minimum energy configuration of the P3HT molecule occurs when the sulfur atom overlaps with the underneath arsenic atom on the GaAs surface and the hexyl chain is aligned along the x axis. This analysis of interfacial configuration of P3HT/GaAs bilayers provides the starting point for further atomic relaxation and calculation of GaAs/P3HT electronic properties.

Electron transfer across GaAs/P3HT interfaces will ultimately determine charge generation efficiency for PV applications. The efficiency of electron transfer mainly depends on the interfacial energy alignment between the conjugated polymer and the inorganic substrate, the electronic couplings between them, and the change of the polymer geometric and electronic structure due to the thermal fluctuations.[23] In experiments, ultrafast pump−probe experiments in GaAs/oligothiophene systems have shown that electron transfer to the conduction band of GaAs occurs upon exciton diffusion toward the heterointerface.[25] In theory, Prezhdo et al. gave detailed time-domain atomistic descriptions of the interfacial charge separation and relaxation processes in hybrid systems.[26] In the case of alizarin/TiO_2 interface, the adiabatic mechanism dominates over nonadiabatic ones due to the strong coupling across the interface.[27] In the case of graphene/TiO_2 interface, electron injection is found to be ultrafast due to the strong electronic coupling between graphene and TiO_2, and both electron injection and energy transfer accelerate for photo-excited states that are delocalized between the two subsystems.[28] An idealized GaAs(10−10)/P3HT interface was investigated theoretically by DFT modeling, showing that the resulting interfacial dipole can lower the highest occupied molecular orbital (HOMO) of the conjugated polymer until the whole system attains equilibrium.[20]

The alignment of the energy levels and the coupling of the electronic wave functions between a polymer and a semiconductor substrate can be obtained from the analysis of the total density of states (DOS) and of the projected density of states (PDOS) after charge redistribution.[29] These are shown for GaAs(110) and (111)B/P3HT interfaces in Figure 2. Figure 2a,a′ shows that the overall DOS of the GaAs and P3HT combined system (black lines) is largely dominated by the projected DOS of GaAs (shaded area), while the projected DOS of P3HT (purple line) only slightly perturbs the top of the valence band of GaAs. States of the P3HT molecule extend over a broad energy range, and there is large overlap between the lowest unoccupied molecular orbital (LUMO) level of P3HT (L_{P3HT}) and the conduction band of GaAs compared with the relatively small overlap of the HOMO of P3HT (H_{P3HT}) and the GaAs valence band. This results in strong electronic coupling between the P3HT molecule and the GaAs. Analysis of the frontier orbitals of the P3HT molecule interacting with the GaAs substrate is carried out to characterize orbital overlap across the interface. Figure 2b,b′,c,c′ shows the spatial distribution of the electron density distribution calculated at the HOMO and LUMO energies of P3HT. Compared with reference bulk GaAs, the bandgap of GaAs(110) slab is lowered as much as 0.4 eV. (See Figure S3 in the Supporting Information.) In the case of GaAs(110)/P3HT, electrons may be efficiently transferred to the bulk of the GaAs crystal thanks to the highly overlapped electron clouds seen at the interface, suggesting the possibility to form hybrid delocalized states. Hole transfer is unfavorable and in any case would be confined to surface states of GaAs(110) due to the poor overlap between the corresponding conduction band and HOMO level.

In the case of the polar GaAs(111)B surface, the DOS is severely affected by the presence of surface dangling bonds (Figure 2b′): As-4p states of the top surface layer and Ga-4p states of the bottom surface layer (not included in the calculations) lie right at the Fermi level inside the bandgap, which results in the appearance of a large number of intragap states and in significant narrowing of the energy bandgap upon lowering of the conduction band energy.[30] The lowering of GaAs(111)B conduction band has a dramatic effect on the relative overlap between GaAs and P3HT states and changes the resulting electron density distribution. In the specific, the conduction band of GaAs(111)B gains overlap with the

dx.doi.org/10.1021/jz401485t | J. Phys. Chem. Lett. 2013, 4, 3303−3309

HOMO of P3HT, facilitating hole transfer from GaAs(111)B to P3HT. Whereas electron transfer from P3HT to GaAs(111)B may be significantly reduced compared with the previous case and somehow confined to the GaAs(111)B surface, holes are allowed to delocalize from the thiophene ring over to the GaAs(111)B surface states and deeply into the bulk thanks to the larger coupling.

To quantify the actual charge transfer and separation processes between polymer and semiconductor substrates, we evaluated the redistribution of charge density upon P3HT adsorption and estimated the changes of interfacial dipole moment and work function that it induces.[31] In organic/inorganic heterojunctions, adsorption of organic molecules on the inorganic substrate is always accompanied by a certain degree of rearrangement of the electronic charge density across the interface; as a consequence, charge transfer between the molecule and the inorganic semiconductor generates a dipole moment that offsets the interfacial potential and reduces the energy level mismatch.[32,33] Thus, the nature of the inorganic surface and its polarity has substantial effects on the formation of interfacial dipoles and may strongly influence charge separation. The electronic charge rearrangement upon formation of the GaAs/P3HT interfaces is shown in Figure 3. The charge transferred from the P3HT molecule to the GaAs substrate was calculated as the difference $\Delta\rho(r) = \rho_{GaAs/P3HT} - [\rho_{GaAs} + \rho_{P3HT}]$, where r is the position vector within the computational cell, ρ_{GaAs} is the charge density of the GaAs(110) and (111)B slabs, ρ_{P3HT} is the charge density of P3HT layer without substrate, and $\rho_{GaAs/P3HT}$ is the electronic charge density of the GaAs/P3HT interface. For both GaAs(110) and GaAs(111)B/P3HT interfaces, adsorption of P3HT onto the substrate induces significant charge transfer, with the formation of distinct charge accumulation layers and substantial charge reorganization at the interface. This indicates the importance of electrostatic interaction between the polymer and the substrate.[34,35] The 1-D plane-averaged charge density difference ($\Delta\rho$) along the z direction shown in Figures 3a,a′ provides quantitative estimate of electron ($\Delta\rho < 0$) and hole ($\Delta\rho > 0$) accumulation, indicating a much larger charge redistribution in the case of the polar GaAs(111)B compared with the nonpolar GaAs(110) surface (up to ~5.3×10^{-3} versus ~0.8×10^{-3} e/Å^3). The main difference between the two surfaces is in the type of charges accumulated at the interface: in the case of nonpolar GaAs(110), holes accumulate both above and below the GaAs surface, while in the case of polar GaAs(111)B, a small electron accumulation layer appears in the top As monolayer. This electron accumulation layer reduces electrostatic screening due to the large interfacial holes density and favors hole transfer from GaAs to P3HT compared with the case of nonpolar GaAs(110).

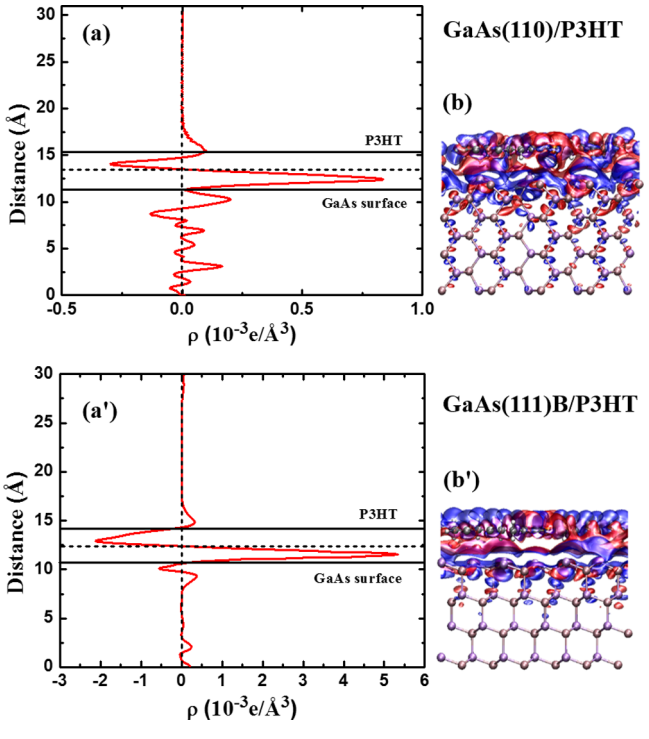

Figure 3. Charge redistribution in GaAs(110)/P3HT (top) and GaAs(111)B/P3HT (bottom) hybrid systems: 1-D plane-averaged charge density difference, $\Delta\rho(z)$, upon P3HT adsorption (a,a′). 3-D representation of the charge density difference with an isovalue of ±0.005 e/Å^3 (b,b′). The solid lines in (a,a′) indicate the average positions of the GaAs surface and the P3HT plane, while the horizontal dashed line shows the interfacial distance at which charge depletion converts into charge accumulation.

The bare GaAs(110) and GaAs(111)B surfaces have distinct polarization properties; although GaAs(110) is usually considered a nonpolar surface, a small intrinsic dipole moment is found due to the tendency of surface Ga atoms to sink toward the bulk, leaving behind an As-terminated surface. The charge-unbalance at the surface forms a negative dipole moment pointing toward the bulk, which, in our simulations, results in a surface charge density of $q_{GaAs(110)} = 2.2 \times 10^{13}$ e/cm^2. Unlike the nonpolar GaAs(110) surface, a large intrinsic dipole moment exists in GaAs(111)B due to the alternating As and Ga terminal layers. In this case, we calculated a surface charge density of $q_{GaAs(111)B} = 7.4 \times 10^{13}$ e/cm^2.[36]

Upon charge redistribution with adsorbed P3HT, the intrinsic surface dipole moment of GaAs surfaces is enhanced by induced charge displacement. A Löwdin charge analysis of the charge density was conducted for these hybrid systems to understand the origin of the interfacial dipole moment.[37] By comparing the sum of the Löwdin charge on the GaAs and P3HT molecule before and after the formation of the interface, a total charge (ΔQ) of 0.207e and 0.209e for GaAs(110)/P3HT and GaAs(111)B/P3HT is found to be transferred between P3HT and GaAs. These charge values are lower than typical organic molecules on metals (Au(111)/naphthalocyanine ≈ 0.7e, Cu(110)/petencene ≈ 0.8e)[38,39] but on the same order of inorganic metal-oxide/polymer interfaces (ZnO/P3HT ≈ 0.3e)[40] and metal-oxide/graphene interface (ZnO/graphene ≈ 0.4e),[41] which are known to induce significant charge transfer.

To validate our simulations, we performed XPS and UPS measurements of the energy alignment of GaAs/P3HT interfaces. According to the integer charge transfer (ICT) model,[42] the energy level alignment of organic/inorganic systems with weak interfacial interactions can be determined from the change of work function upon adsorption of the organic molecule. Removing charges from conjugated polymer can induce substantial geometric and electronic relaxation effects, which leads to localized positive polaronic states (p+).[43] If the work function of substrate (Φ_{SUB}) is larger than the energy of the polaronic states (E_{p+}), then electrons will spontaneously transfer from the organic layer into the inorganic substrate, creating a dipole that reduces the vacuum level, where the interfacial dipole energy (Δ) caused by charge

dx.doi.org/10.1021/jz401485t | J. Phys. Chem. Lett. 2013, 4, 3303−3309

redistribution can be obtained from the energy difference between the Φ_{SUB} and E_{p+}.

The position of the HOMO level of P3HT is determined to be 1.10 and 0.64 eV below the Fermi energy from the Fermi-edge regions of UPS spectra of P3HT-coated GaAs(110) and GaAs(111)B substrates (Figures S4a,c in the Supporting Information). Meanwhile, from the cutoff of the UPS spectra (Figure S5a,c in the Supporting Information), the work function of P3HT on GaAs(100) and GaAs(111)B substrates ($\Phi_{P3HT/SUB}$) is found to be 3.78 and 4.00 eV, respectively. Care was taken to effectively remove the surface oxide layer before deposition of P3HT in an inert argon-gas atmosphere by treating the GaAs substrates with H_2SO_4 solution. This is substantiated by the absence of Ga_2O_3 and As_2O_3 peaks in the XPS spectra of the substrates. (See Figure S6 in the Supporting Information.) To determine the energetics of the bare substrates, the thin P3HT films were removed in situ by Ar ion sputtering until exposure of clean GaAs surfaces. GaAs(110) and GaAs(111)B substrates showed the valence band maxima (VBM) of 0.69 and 0.68 eV (shown in Figures S4b,d in the Supporting Information) and work functions of 4.76 and 4.95 eV (as obtained from the onset of the UPS spectra in Figure S5b,d in the Supporting Information). The LUMO level of P3HT is determined by adding the optical gap energy (1.9 eV) to the HOMO; similarly, the CBM of GaAs is the sum of VBM and GaAs optical gap energy (1.42 eV).

The overall picture of energy level alignment determined by the above measurements is sketched in Figures 4a,a′. A nested configuration (type I) is obtained at the GaAs(110)/P3HT interface, whereas a staggered band alignment (type II) is observed in the GaAs(111)B/P3HT case, which agrees well with the calculated energy alignment in Figure 2a,a′. Both configurations favor electron transfer from P3HT to GaAs substrates because of the barrier between conduction band minimum (CBM) of GaAs and LUMO of the P3HT film. The higher work function of bare GaAs substrates compared with the hybrid GaAs/P3HT systems can be attributed to the build up of interfacial dipole barrier of −0.98 and −0.95 eV, respectively, which results from the displacement of negative charge from P3HT film to GaAs substrates. Only in the case of GaAs(111)B is the valence level offset favorable for hole injection from the P3HT layer ($E_{HOMO} - E_{VBM}$ = 0.04 eV), suggesting that P3HT could act as a "hole acceptor"; opposite behavior is expected for the GaAs(110) surface. The vacuum level shift induced by the interfacial dipole, $\Delta\Phi$, can be calculated from the comparison of the electrostatic potential between the GaAs surface and the P3HT molecular plane using the Helmholtz equation $\Delta\Phi = \mu n/\varepsilon_0$.[31] (Here μ is the interface dipole moment, that is, the amount of excess of charge obtained from Löwdin charge analysis multiplied by the interfacial distance, n = 1/A, where A is the surface area of the interface.) Because only one monolayer of P3HT was considered in the simulations, the values of $\Delta\Phi$ = 0.769 and 0.868 eV obtained for the GaAs(111)B and GaAs(110) are slightly lower than the interfacial dipole barriers observed experimentally. Preliminary findings from ultrafast spectroscopy measurements in organic−inorganic bilayers confirm these predictions: upon photoexcitation of P3HT, fast (<100 fs) electron transfer takes place from P3HT to GaAs(111)B and GaAs(110) substrates, and convincing signatures of hole transfer to P3HT are also observed by energy-selective excitation of GaAs. (These results are about to be published elsewhere.)

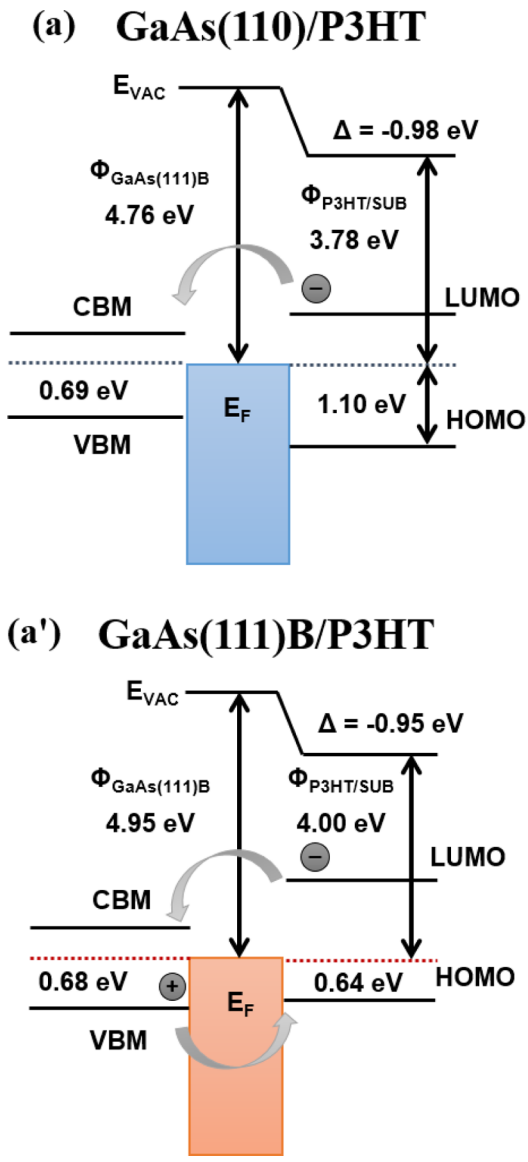

Figure 4. Schematic of the energy diagrams determined from UPS measurements of GaAs(110)/P3HT (a) and GaAs(111)B/P3HT (a′) heterointerfaces.

In summary, we performed DFT calculations to investigate the atomic configurations and electronic properties of GaAs/P3HT organic−inorganic hybrid systems. We find that the different polarity of the GaAs surface states shows different electronic orbital and charge redistribution properties. Both cases favor electron transfer from P3HT to GaAs substrates. GaAs(111)B surface tends to facilitate hole transfer from the VB states to HOMO of P3HT that acts as a "hole acceptor". Enhanced surface dipole moments of GaAs surfaces induce charge transfer ($\Delta Q \approx 0.21e$) for both GaAs(110)/P3HT and GaAs(111)B/P3HT. The results of our calculations correlate well with experimental observations made by UPS and ultrafast spectroscopy measurements and are significant for the fundamental understanding and the design of hybrid PV systems based on the combination of organic and inorganic semiconductors.

dx.doi.org/10.1021/jz401485t | J. Phys. Chem. Lett. 2013, 4, 3303−3309

EXPERIMENTAL METHODS

Computational Method. Density functional theory (DFT) with local density approximation (LDA) functional[44] calculations were carried out using the Quantum-ESPRESSO software package.[37] The ultrasoft (C, S, and H atoms) and norm-conserving of (Ga and As atoms) pseudopotentials were used to describe the electron-ion interactions. The electronic wave functions and charge density were expanded with an energy cutoff of 40 and 320 Ry, respectively. The vdW-DF functional[45] that accounts for dispersion effects self-consistently was also used for structural and electronic calculations because dispersion forces have a significant additive stabilization effect on CT systems. For calculations of bulk GaAs, the integration over the Brillouin zone was performed using a *k*-points grid of 8 × 8 × 8 during the cell optimization and electronic properties calculations. We have obtained a lattice constant of a = 5.543 Å, which is close to the experimental value of a = 5.653 Å. GaAs(110) and (111)B surface orientations were selected to study the effects of surface polarity; they are stable surfaces observed in the experiments,[46,47] and both top layers terminate with As atoms. For the calculations of the GaAs slabs, in-plane lattice parameters of GaAs(110) and GaAs(111)B surfaces were obtained from optimization of the corresponding bulk GaAs. The corresponding surfaces were represented by periodically repeated 4 × 2 surface supercells originated from common GaAs(110) (1 × 1) and GaAs(111)B (2 × 1) surface reconstructions. Each slab layer contains four bilayers, where atomic positions in the bottom bilayer are fixed to mimic the bulk GaAs while the other layers are fully relaxed. A vacuum region of ∼15 Å was added to avoid interaction between neighboring slabs. For the calculations of crystalline P3HT, the polymer structure was determined from a repeat unit containing two thiophene rings. The 4 × 2 GaAs(110) and (111)B surface supercells combined with the P3HT crystal two repeated unit (no interdigitation of alkyl side chain) were used to model interfacial structure. The transverse areas of the GaAs(110) and (111)B slabs are 22.17 × 7.70 and 20.37 × 7.66 Å^2, respectively. A 4 × 4 × 1 *k*-point grid was used to study clean GaAs(110) and (111)B surfaces and GaAs/P3HT interfaces. All surface and interface geometries were optimized with the method of Broyden−Fletcher−Goldfarb−Shanno (BFGS) until all of the forces on all atoms became lower than 0.02 eV/Å and total energy difference between two optimization steps of the minimization procedures was $<10^{-4}$ eV. All of the 3-D representations of charge density are produced by VMD.[48] The surface energy is defined as $E_{surf} = (1/2A)[E_{slab} - nE_{bulk}]$,[49] where E_{surf} is the total energy of the surface, n is the total number of atoms in the slab, E_{bulk} is the energy per atom of the bulk structure, and A is the area of the surface.

XPS and UPS Spectroscopy. X-ray and ultraviolet photoelectron spectroscopy (XPS and UPS) are used to investigate the energy level alignments of GaAs/P3HT interfaces. *n*-doped GaAs(111)B and (110) substrates were chemically etched with diluted H_2SO_4/H_2O 1:10 solution. P3HT was dissolved in 1,2-dichlorobenzene (4 mg/mL) and spin-coated on the GaAs substrates at 3000 rpm for 60 s. The resulting polymer film thickness was determined to be 5−7 nm by atomic force microscopy. After deposition the samples were thermally annealed at 150 °C for 20 min under an inert atmosphere of Ar gas. XPS and UPS measurements were performed under high vacuum with excitations of Al Kα ($h\nu$ = 1486.7 eV) and He I ($h\nu$ = 21.2 eV).

ASSOCIATED CONTENT

Supporting Information

Changes in binding energy and UPS and XPS spectra of thin P3HT film on GaAs(110) and GaAs(111)B substrates. This material is available free of charge via the Internet at http://pubs.acs.org.

AUTHOR INFORMATION

Corresponding Author

*E-mail: csoci@ntu.edu.sg.

Notes

The authors declare no competing financial interest.

ACKNOWLEDGMENTS

Research was supported by the NTU NAP startup grant (no. M4080511) and by the Funding of Initiatives in Support of NTU 2015 (no. M58110092). We thank Alfred Huan for his help with UPS and XPS measurements and Guglielmo Lanzani, Francesco Scotognella, and Daniele Fazzi for the useful discussions regarding this work.

REFERENCES

(1) Huynh, W. U.; Dittmer, J. J.; Alivisatos, A. P. Hybrid Nanorod-Polymer Solar Cells. *Science* **2002**, *295*, 2425−2427.
(2) Yin, Y.; Alivisatos, A. P. Colloidal Nanocrystal Synthesis and the Organic-Inorganic Interface. *Nature* **2005**, *437*, 664−670.
(3) Liu, C. Y.; Holman, Z. C.; Kortshagen, U. R. Hybrid Solar Cells from P3HT and Silicon Nanocrystals. *Nano Lett.* **2009**, *9*, 449−452.
(4) Chang, J. A.; Rhee, J. H.; Im, S. H.; Lee, Y. H.; Kim, H. J.; Seok, S. I.; Nazeeruddin, M. K.; Gratzel, M. High-Performance Nanostructured Inorganic-Organic Heterojunction Solar Cells. *Nano Lett.* **2010**, *10*, 2609−2612.
(5) Dayal, S.; Kopidakis, N.; Olson, D. C.; Ginley, D. S.; Rumbles, G. Photovoltaic Devices with a Low Band Gap Polymer and CdSe Nanostructures Exceeding 3% Efficiency. *Nano Lett.* **2010**, *10*, 239−242.
(6) Vaynzof, Y.; Kabra, D.; Zhao, L. H.; Ho, P. K. H.; Wee, A. T. S.; Friend, R. H. Improved Photoinduced Charge Carriers Separation in Organic-Inorganic Hybrid Photovoltaic Devices. *Appl. Phys. Lett.* **2010**, *97*, 033309−033312.
(7) Vanlaeke, P.; Swinnen, A.; Haeldermans, I.; Vanhoyland, G.; Aernouts, T.; Cheyns, D.; Deibel, C.; D'Haen, J.; Heremans, P.; Poortmans, J.; et al. P3HT/PCBM Bulk Heterojunction Solar Cells: Relation between Morphology and Electro-Optical Characteristics. *Sol. Energy Mater. Sol. Cells* **2006**, *90*, 2150−2158.
(8) Duhm, S.; Heimel, G.; Salzmann, I.; Glowatzki, H.; Johnson, R. L.; Vollmer, A.; Rabe, J. P.; Koch, N. Orientation-Dependent Ionization Energies and Interface Dipoles in Ordered Molecular Assemblies. *Nat. Mater.* **2008**, *7*, 326−332.
(9) Bassani, F.; La Rocca, G. C.; Basko, D. M.; Agranovich, V. M. Excitons in Hybrid Organic-Inorganic Nanostructures. *Phys. Solid State* **1999**, *41*, 701−703.
(10) Blumstengel, S.; Sadofev, S.; Xu, C.; Puls, J.; Henneberger, F. Converting Wannier into Frenkel Excitons in an Inorganic/Organic Hybrid Semiconductor Nanostructure. *Phys. Rev. Lett.* **2006**, *97*, 237401−237404.
(11) Zhang, Q.; Atay, T.; Tischler, J. R.; Bradley, M. S.; Bulovic, V.; Nurmikko, A. V. Highly Efficient Resonant Coupling of Optical Excitations in Hybrid Organic/Inorganic Semiconductor Nanostructures. *Nat. Nanotechnol.* **2007**, *2*, 555−559.
(12) Nizamoglu, S.; Sun, X. W.; Demir, H. V. Observation of Efficient Transfer from Mott-Wannier to Frenkel Excitons in a Hybrid

Semiconductor Quantum Dot/Polymer Composite at Room Temperature. *Appl. Phys. Lett.* **2010**, *97*, 263106−263108.
(13) Yong, C. K.; Joyce, H. J.; Lloyd-Hughes, J.; Gao, Q.; Tan, H. H.; Jagadish, C.; Johnston, M. B.; Herz, L. M. Ultrafast Dynamics of Exciton Formation in Semiconductor Nanowires. *Small* **2012**, *8*, 1725−1731.
(14) Yablonovitch, E.; Miller, O. D.; Kurtz, S. R. The Opto-Electronic Physics That Broke the Efficiency Limit in Solar Cells. *IEEE Photovoltaic Spec. Conf., 38th* **2012**, 1556−1559.
(15) Ackermann, J.; Videlot, C.; El Kassmi, A. Growth of Organic Semiconductors for Hybrid Solar Cell Application. *Thin Solid Films* **2002**, *403*, 157−161.
(16) Ren, S. Q.; Zhao, N.; Crawford, S. C.; Tambe, M.; Bulovic, V.; Gradecak, S. Heterojunction Photovoltaics Using GaAs Nanowires and Conjugated Polymers. *Nano Lett.* **2011**, *11*, 408−413.
(17) Chao, J. J.; Shiu, S. C.; Lin, C. F. GaAs Nanowire/Poly(3,4-ethylenedioxythiophene):Poly(styrenesulfonate) Hybrid Solar Cells with Incorporating Electron Blocking Poly(3-hexylthiophene) Layer. *Sol. Energy Mater. Sol. Cells* **2012**, *105*, 40−45.
(18) Mariani, G.; Laghumavarapu, R. B.; de Villers, B. T.; Shapiro, J.; Senanayake, P.; Lin, A.; Schwartz, B. J.; Huffaker, D. L. Hybrid Conjugated Polymer Solar Cells Using Patterned GaAs Nanopillars. *Appl. Phys. Lett.* **2010**, *97*, 013107−013109.
(19) Yan, L.; You, W. Real Function of Semiconducting Polymer in GaAs/Polymer Planar Heterojunction Solar Cells. *ACS Nano* **2013**, *7*, 6619−6626.
(20) Yong, C. K.; Noori, K.; Gao, Q.; Joyce, H. J.; Tan, H. H.; Jagadish, C.; Giustino, F.; Johnston, M. B.; Herz, L. M. Strong Carrier Lifetime Enhancement in GaAs Nanowires Coated with Semiconducting Polymer. *Nano Lett.* **2012**, *12*, 6293−6301.
(21) Qian, G. X.; Richard, M. M.; Chadi, D. J. First-Principles Calculations of Atomic and Electronic Structure of the GaAs(110) Surface. *Phys. Rev. B* **1988**, *37*, 1303−1307.
(22) Yi, Z. J.; Ma, Y. C.; Rohlfing, M. Silicon Donors at the GaAs(110) Surface: A First Principles Study. *J. Phys. Chem. C* **2011**, *115*, 23455−23462.
(23) Dag, S.; Wang, L. W. Modeling of Nanoscale Morphology of Regioregular Poly(3-hexylthiophene) on a ZnO (10−10) Surface. *Nano Lett.* **2008**, *8*, 4185−4190.
(24) Calzolari, A.; Ruini, A.; Catellani, A. Surface Effects on Catechol/Semiconductor Interfaces. *J. Phys. Chem. C* **2012**, *116*, 17158−17163.
(25) Cabanillas-Gonzalez, J.; Gambetta, A.; Zavelani-Rossi, M.; Lanzani, G. Kinetics of Interfacial Charges in Hybrid GaAs/Oligothiophene Semiconducting Heterojunctions. *Appl. Phys. Lett.* **2007**, *91*, 122113−122115.
(26) Akimov, A. V.; Neukirch, A. J.; Prezhdo, O. V. Theoretical Insights into Photoinduced Charge Transfer and Catalysis at Oxide Interfaces. *Chem. Rev.* **2013**, *113*, 4496−4565.
(27) Duncan, W. R.; Craig, C. F.; Prezhdo, O. V. Time-Domain Ab Initio Study of Charge Relaxation and Recombination in Dye-Sensitized TiO2. *J. Am. Chem. Soc.* **2007**, *129*, 8528−8543.
(28) Long, R.; English, N. J.; Prezhdo, O. V. Photo-Induced Charge Separation across the Graphene-TiO2 Interface Is Faster Than Energy Losses: A Time-Domain Ab Initio Analysis. *J. Am. Chem. Soc.* **2012**, *134*, 14238−14248.
(29) Nenon, S.; Mereau, R.; Salman, S.; Castet, F. Structural and Electronic Properties of the TTF/ZnO(10−10) Interface: Insights from Modeling. *J. Phys. Chem. Lett.* **2012**, *3*, 58−63.
(30) Lin, L.; Robertson, J. Defect States at III-V Semiconductor Oxide Interfaces. *Appl. Phys. Lett.* **2011**, *98*, 082903−082905.
(31) Sai, N.; Gearba, R.; Dolocan, A.; Tritsch, J. R.; Chan, W. L.; Chelikowsky, J. R.; Leung, K.; Zhu, X. Y. Understanding the Interface Dipole of Copper Phthalocyanine (CuPc)/C-60: Theory and Experiment. *J. Phys. Chem. Lett.* **2012**, *3*, 2173−2177.
(32) Ishii, H.; Sugiyama, K.; Ito, E.; Seki, K. Energy Level Alignment and Interfacial Electronic Structures at Organic/Metal and Organic/Organic Interfaces. *Adv. Mater.* **1999**, *11*, 972−972.
(33) Crispin, X.; Geskin, V.; Crispin, A.; Cornil, J.; Lazzaroni, R.; Salaneck, W. R.; Bredas, J. L. Characterization of the Interface Dipole at Organic/Metal Interfaces. *J. Am. Chem. Soc.* **2002**, *124*, 8131−8141.
(34) Nemec, H.; Rochford, J.; Taratula, O.; Galoppini, E.; Kuzel, P.; Polivka, T.; Yartsev, A.; Sundstrom, V. Influence of the Electron-Cation Interaction on Electron Mobility in Dye-Sensitized ZnO and TiO2 Nanocrystals: A Study Using Ultrafast Terahertz Spectroscopy. *Phys. Rev. Lett.* **2010**, *104*, 197401−197404.
(35) Monti, O. L. A. Understanding Interfacial Electronic Structure and Charge Transfer: An Electrostatic Perspective. *J. Phys. Chem. Lett.* **2012**, *3*, 2342−2351.
(36) Bernardini, F.; Fiorentini, V.; Vanderbilt, D. Spontaneous Polarization and Piezoelectric Constants of III-V Nitrides. *Phys. Rev. B* **1997**, *56*, 10024−10027.
(37) Giannozzi, P.; Baroni, S.; Bonini, N.; Calandra, M.; Car, R.; Cavazzoni, C.; Ceresoli, D.; Chiarotti, G. L.; Cococcioni, M.; Dabo, I.; et al. Quantum Espresso: A Modular and Open-Source Software Project for Quantum Simulations of Materials. *J. Phys.: Condens. Matter* **2009**, *21*, 395502−395520.
(38) Terentjevs, A.; Steele, M. P.; Blumenfeld, M. L.; Ilyas, N.; Kelly, L. L.; Fabiano, E.; Monti, O. L. A.; Della Sala, F. Interfacial Electronic Structure of the Dipolar Vanadyl Naphthalocyanine on Au(111): "Push-Back" Vs Dipolar Effects. *J. Phys. Chem. C* **2011**, *115*, 21128−21138.
(39) Muller, K.; Seitsonen, A. P.; Brugger, T.; Westover, J.; Greber, T.; Jung, T.; Kara, A. Electronic Structure of an Organic/Metal Interface: Pentacene/Cu(110). *J. Phys. Chem. C* **2012**, *116*, 23465−23471.
(40) Noori, K.; Giustino, F. Ideal Energy-Level Alignment at the ZnO/P3HT Photovoltaic Interface. *Adv. Funct. Mater.* **2012**, *22*, 5089−5095.
(41) Geng, W.; Z., X. F.; Liu, H. X.; Yao, X. J. Influence of Interface Structure on the Properties of ZnO/Graphene Composites: A Theoretical Study by Density Functional Theory Calculations. *J. Phys. Chem. C* **2013**, *117*, 10536−10544.
(42) Braun, S.; Salaneck, W. R.; Fahlman, M. Energy-Level Alignment at Organic/Metal and Organic/Organic Interfaces. *Adv. Mater.* **2009**, *21*, 1450−1472.
(43) Xu, Z.; Chen, L. M.; Chen, M. H.; Li, G.; Yang, Y. Energy Level Alignment of Poly(3-hexylthiophene): [6,6]-Phenyl C-61 Butyric Acid Methyl Ester Bulk Heterojunction. *Appl. Phys. Lett.* **2009**, *95*, 013301−013303.
(44) Perdew, J. P.; Zunger, A. Self-Interaction Correction to Density-Functional Approximations for Many-Electron Systems. *Phys. Rev. B* **1981**, *23*, 5048−5079.
(45) Dion, M.; Rydberg, H.; Schroder, E.; Langreth, D. C.; Lundqvist, B. I. van der Waals Density Functional for General Geometries. *Phys. Rev. Lett.* **2004**, *92*, 246401−246404.
(46) Ohtake, A.; Nakamura, J.; Komura, T.; Hanada, T.; Yao, T.; Kuramochi, H.; Ozeki, M. Surface Structures of GaAs{111}a,B-(2 × 2). *Phys. Rev. B* **2001**, *64*, 45318−45325.
(47) Skeath, P.; Saperstein, W. A.; Pianetta, P.; Lindau, I.; Spicer, W. E.; Mark, P. Ups and Leed Studies of GaAs (110) and (111) as Surfaces. *J. Vac. Sci. Technol.* **1978**, *15*, 1219−1222.
(48) Humphrey, W.; Dalke, A.; Schulten, K. VMD: Visual Molecular Dynamics. *J. Mol. Graphics Modell.* **1996**, *14*, 33−38.
(49) D'Amico, N. R.; Cantele, G.; Ninno, D. First-Principles Calculations of Clean and Defected ZnO Surfaces. *J. Phys. Chem. C* **2012**, *116*, 21391−21400.